Physicochemical Studies of Tamarind Shell Tannins as a Potential Green Rust Converter

Abdullahi Abdulmajid,[a,b] Tuan Sherwyn Hamidon,[b] Afidah Abdul Rahim,[b] and M. Hazwan Hussin [b,*]

The characterization of tamarind shell tannins for potential use in rust transformation was studied. Fourier-transform infrared spectroscopy (FTIR), nuclear magnetic resonance (NMR), differential scanning calorimetry (DSC), thermal gravimetric analysis (TGA), and phytochemical assays were applied to examine tamarind shell tannins. The analyses revealed that the methanol extract of tamarind shell (TME) was rich in phytochemical compounds, compared to that of aqueous acetone extract of tamarind shell (TAE). Furthermore, the FTIR and NMR studies confirmed the presence of tannins. The FTIR study on the performance of tamarind shell tannins on rust treatment *via* the effects of concentration, pH, and reaction time was evaluated. The FTIR spectra revealed that the percentage rust transformation (RT %) was in the order of lepidocrocite (γ-FeOOH) > magnetite (Fe_3O_4) > goethite (α-FeOOH). Meanwhile, the results obtained revealed that lepidocrocite peaks completely disappeared, and magnetite peaks reduced intensity up to 95.83 RT % for TME and 94.75 RT % for TAE. The TME was the best rust converter at 7% concentration.

Keywords: Tamarind shell; Tannin; Rust converter

*Contact information: a: Hassan Usman Katsina Polytechnic, Katsina, 2052 Nigeria; b: Materials Technology Research Group (MaTReC), School of Chemical Sciences, Universiti Sains Malaysia, 11800 Minden, Penang, Malaysia; *Corresponding author: mhh@usm.my; mhh.usm@gmail.com*

INTRODUCTION

Tannins are higher plants' secondary polyphenolic metabolites, which are derivatives of galloyl esters, in which their galloyl moieties are attached to a range of catechin, polyol, and triterpenoid centers. Based on their structural characteristics, tannins are therefore divided into four major groups: ellagitannins, gallotannins, condensed tannins, and complex tannins. Ellagitannins are tannins with two galloyl units attached to one another through C–C bonds, and they do not contain a glycosidic catechin linkage unit. Gallotannins are tannins in which their galloyl units or their derivatives are linked to various catechins, polyols, or units of triterpenoid. Complex tannins are tannins in which ellagitannin and a gallotannin unit are glycosidically linked to a catechin unit. Oligomeric and polymeric proanthocyanidins are condensed tannins that are formed through C4 linkage of one catechin monomer with C8 or C6 of another catechin monomer (Khanbabaee and van Ree 2001).

Tannins have been known since ancient times as organic substances that are able to convert animal skins into leather (Khanbabaee and van Ree 2001). High concentrations of tannins are present in almost every portion of plants, including leaves, bark, wood, roots, fruits, and seeds (Haslam 1989; Balasundram *et al*. 2006). They are widely used in the production of cationic dyes, iron gallate ink, clarifying agents in wine, textile dyes,

fruit juice antioxidants, and coagulants in the production of rubber (Khanbabaee and van Ree 2001). They are able to form complexes with various substances and precipitate in aqueous solution (Lokeswari and Sujatha 2011). This leads to their recent industrial applications as flocculants, adhesives, depressants, corrosion inhibitors, viscosity modifying agents, and rust converters. Thus, they have become important raw materials for industrial purposes (Rahim *et al.* 2011). They have been used as rust converters because they can complex with active hydrated iron oxides such as lepidocrocite (γ-FeOOH), goethite (α-FeOOH), and magnetite (Fe_3O_4) into ferric tannates. Rust converters are chemicals that can be applied on a corroded steel surface to convert rust into an insoluble and adherent black film of chemical compounds (Zhao *et al*. 2014). It has been found that the rust converters can convert the iron rust into a transformation film, aiding as a barrier cover to block corrosive species from reaching the iron or steel surface. This barrier slows down the redox reactions of the metal and then decreases the deterioration of the protective system (Pereyra *et al*. 2006).

However, due to the ortho-position of OH- group on the aromatic rings, tannins compounds are capable of forming complexes with metallic cations and iron (Mabrour *et al.* 2004). Previous studies reported the formation of ferric tannate with hydrolysable and condensed tannins (Yahya *et al*. 2008). Moreover, when an OH-group of the ortho-position on aromatic rings reacts with Fe^{3+} ions in aqueous solution, a highly insoluble and blue-black complex of ferric tannate is formed (Gust and Suwalski 1994). The ferric tannate serves as a protective chemical barrier that protects the surface of the steel or iron from corrosion. The ferric tannates' efficiency in protection against further corrosion is not generally established based on the different materials used in various studies (Rahim *et al*. 2011). Earlier studies have evaluated oak tannin (Gust 1991; Gust and Bobrowicz 1993), gallic acid (Rahim *et al*. 2011), tannic acid (Favre and Landolt 1993; Feliu *et al*. 1993; Nasrazadani 1997; Barrero *et al.* 2001), mimosa tannin (Ross and Francis 1978), and pine tannin (Matamala *et al.* 2000). Corrosion inhibition studies have shown an excellent inhibition efficiency of mangrove bark tannin in acidic media. With an increase in pH, the inhibition efficiency decreases. At low pH, the mechanism of inhibition is the chemisorption of tannin molecules, while at greater pH (2 to 4), the transformation results in the formation of ferric tannates (Rahim *et al*. 2011).

Tamarind (*Tamarindus indica*) trees are abundant in Africa and Southeast Asia. These trees contain numerous brown pods with brown seeds bounded by a gummy pulp that dries naturally to a sticky paste. The sticky paste is commonly used as a flavouring agent in various cuisines because of its characteristic taste (Mercola 2015). However, the shells are not commonly utilized and are regarded as wastes. Thus, the potential utilization of this waste biomass material has become important. Despite growing interest, although it seems that tamarind *(Tamrindus indica* L.) shells contain polyphenolic compounds, (Luengthanaphol *et al.* 2004; Sudjaroen *et al*. 2005), the quantification of the phytochemical components and the characterization, such as thermal stability of the shell extract has not been fully investigated, and there has been a lack of published information concerning application of the tamarind shell tannin extract for rust transformation. Therefore, this study aimed at characterizing tamarind shell tannins from two solvent extracts (methanol and aqueous acetone) by complementary analyses such as Fourier-transform infrared (FTIR) spectroscopy, ^{1}H and ^{13}C nuclear magnetic resonance (NMR) spectroscopy, differential scanning calorimetry (DSC), and thermal gravimetric analysis (TGA). Rust conversion studies and specific optimizations were performed in assistance of FTIR spectroscopy.

EXPERIMENTAL

Materials and Methods

Extraction of tamarind shell tannins

Shells of tamarind were collected from Katsina state, Nigeria, in mid-2017. The shells were ground into a powder and sieved through a 250-µm mesh. Approximately 10 g of powdered sample was mixed with 100 mL of methanol and incubated for 24 h at ambient room temperature (28 °C ± 2 °C) at 145 rpm under maceration. Then, the solution was filtered using vacuum filtration, and the extraction was repeated twice, each time with 100 mL of methanol. Upon filtration, the combined tannin methanol extracts (TME) were concentrated under reduced pressure by rotary evaporation (4011 digital, Heidolph Instruments, Schwabach, Germany), and the resulting solution was dried at 50 °C overnight to obtain a dark green extract, which was kept in a refrigerator for further use. The process was repeated using 70% acetone solution. The resulting tannin acetone crude extract (TAE) was freeze-dried upon rotary evaporation to obtain a brown powdered extract (Rahim *et al*. 2011).

Physicochemical Characterization

Fourier transform infrared (FTIR) spectroscopy

The IR spectra of both the TME and TAE were recorded using a Perkin Elmer System 2000 (Waltham, MA, USA), with a wavelength range of 4000 cm^{-1} to 400 cm^{-1} at 4 cm^{-1} resolution and 16 scans. The potassium bromide technique (KBr) was applied to the samples with the proportion of 1:20 (w/w).

Nuclear magnetic resonance (NMR) spectroscopy

Approximately 150 mg of the TME and TAE samples were dissolved in 0.4 mL of dimethyl sulfoxide (DMSO) and injected into an NMR tube. A Bruker Avance 500 MHz spectrometer (Fallanden, Switzerland) was used to perform the analysis at 50 °C overnight. The spectra were analysed using Bruker Top Spin software (3.5, Oxford, U.K).

Thermal gravimetric analysis (TGA)

A Perkin Elmer TGA 7 thermogravimetric analyzer (Waltham, MA, USA) recorded the thermal stability of 5 mg samples of the TME and TAE from 30 °C to 900 °C with a 10 °C min^{-1} heating rate under nitrogen atmosphere.

Differential scanning calorimetry (DSC)

A Perkin Elmer Pyris 1 (Waltham, MA, USA) was used to perform the DSC analysis, where 5 mg samples were heated from 30 °C to 200 °C with a 10 °C min^{-1} heating rate.

Phytochemical Assays

Total phenolic content (TPC)

The Folin-Ciocalteu reagent method was used to determine total phenolic content with gallic acid as a standard (McDonald *et al*. 2001). A volume of 0.5 mL of each extract (10:100, w/v) and standard gallic acid (Fluka, Steinheim.Germany) was mixed with 5 mL of Folin-Ciocalteu reagent (Merck, Darmstadt, Germany) (10:100, v/v distilled water) and 4 mL of 1 M aqueous Na_2CO_3 (QRec, Selangor, Malaysia). Concentrations of 20 ppm, 40 ppm, 60 ppm, 80 ppm, and 100 ppm gallic acid standard solutions were

prepared, and the absorbance of each mixture was measured at 765 nm (UV-2600, Shimadzu, Kyoto, Japan) after keeping them for 2 h in dark surroundings. Total phenolic content was expressed in terms of gallic acid equivalent, GAE (mg g^{-1}).

Total flavonoid content (TFC)

First, 1.0 mL of each extract (0.5 g of extract in 50 mL of methanol) was added into a volumetric flask (10 mL) comprising 4 mL of distilled water. Then, 0.3 mL of 5% $NaNO_3$ (Merck) was added to the flask, and 0.3 mL of 10% $AlCl_3$ (Systerm, Kuala Lumpur, Malaysia) was added after 5 min. At 6 min, 2.0 mL of 1 M NaOH (QRec, Selangor, Malaysia) solution was added, and the total volume (10 mL) was made up with distilled water. The absorbance was measured at 510 nm against the prepared reagent blank after mixing the solution. A standard solution of (+)-catechin hydrate (Sigma-Aldrich, St. Louis, MO, USA) ranging from 10 ppm to 100 ppm was used to plot the calibration curve. Total flavonoid content was expressed in terms of catechin mg g^{-1} equivalent (CE) (Kassim *et al*. 2011).

Total tannin content (TTC)

The proposed method by Garro-Gavlez *et al*. (1996) and Yazaki (1985) after a slight modification was applied for the total condensed tannin determination in sample extracts. First, 100 mg of each sample extract was dissolved in 10 mL of distilled water. Next, 2 mL of 37% formaldehyde (Merck, Darmstadt, Germany) and 2 mL of 5 M HCl were added into the mixture, and the mixture was heated under reflux for 1 h. Vacuum suction was used to filter the reaction mixture while it was hot. A volume of 10 mL of hot water was used to wash the reddish precipitate 5 times. The precipitate was then dried in a desiccator and weighed. The percentage weight of the starting material was expressed as the yield.

Rust Conversion Studies

Preparation of rust powder

Mild steel plates with elemental compositions of 0.01 wt% C, 0.16 wt% Si, 0.15 wt% Mn, 0.01 wt% P, 0.06 wt.% Al, 0.02 wt.% Na, 0.03 wt.% Mg, and balance Fe were used. The plates (12 cm × 8 cm × 0.1 cm) were cleaned with 100, 200, 400, 600, and 800 grades SiC papers, rinsed with distilled water and acetone, and dried at ambient room temperature (28 °C ± 2 °C). The plates were then exposed in a salt spray chamber (TERCHY Salt Spray Tester SST-12MS, Dongguan Terchy Test Equipment Co. Ltd, Dongguan, China) containing 5% NaCl (QRec, Selangor, Malaysia) for 6 h according to the ASTM B117 standard (test room temperature: 33°C ± 1 °C, standard air temperature: 35 °C ± 1 °C, air pressure: 98.1 kPa, spray rate: 1 mL min^{-1}). The plates were then rinsed with distilled water and dried in an oven at 50 °C overnight. The produced rust was removed with a scraper, ground into a powder, and kept in a closed container for further studies.

FTIR analysis of rust

The IR spectra of both the salt-spray-generated rust and the rust standards (Fe_3O_4 magnetite, γ-FeOOH lepidocrocite, and α-FeOOH goethite, Sigma-Aldrich, St. Louis, MO, USA) were recorded using a Perkin Elmer System 2000 (Waltham, MA, USA), with a wavelength range of 4000 cm^{-1} to 400 cm^{-1} at 4 cm^{-1} resolution and 16 scans. The

potassium bromide technique (KBr, Uvasol, Darmstadt, Germany) was applied with the proportion of 1:20 (w/w).

Effect of concentration

Rust powder (50 mg) was mixed with 1 wt%, 3 wt%, 5 wt%, and 7 wt% of, each, TME and TAE, 25 mL of isopropyl alcohol, and 75 mL of distilled water. The pH of the solutions was adjusted to 5, and the mixtures were incubated at ambient room temperature 28 °C ± 2 °C for 24 h at 145 rpm under maceration. Next, the mixture was filtered, and the precipitate residue was dried in an oven at 50 °C overnight. The dried precipitate was analyzed with the FTIR spectrometer.

Effect of pH

Rust powder (50 mg) was mixed with 7 wt% of, each, TME and TAE, 25 mL of isopropyl alcohol, and 75 mL of distilled water. The pH of the solutions was varied according to the pH values of 1, 3, 5, 7, 9, and 11, with the mixture incubated at ambient room temperature for 24 h at 145 rpm under maceration. Next, the mixture was filtered, and the precipitate residue was dried in an oven at 50 °C overnight. The dried precipitate was analyzed with the FTIR spectrometer.

Effect of reaction time

Rust powder (50 mg) was mixed with 7 wt% of, each, TME and TAE, 25 mL of isopropyl alcohol, and 75 mL of distilled water. The pH of the solutions was adjusted to 3, and the mixture was incubated for 1 d, 3 d, 5 d, 7 d, and 14 d at ambient room temperature at 145 rpm under maceration. Then, the mixture was filtered, and the precipitate residue was dried in an oven at 50 °C overnight. The dried precipitate was analyzed with the FTIR spectrometer.

RESULTS AND DISCUSSION

The percentage yield of tamarind shell extract using the methanol solvent (TME) (18.66%) was greatest, followed by the acetone solvent (TAE) (17.33%). There was a slight difference between the yields of the extracts. Based on these percentage yields for the extraction, methanol was a better medium than acetone. However, choices of extraction techniques, solvent medium, and varying parameters such as time, temperature, and pH might play an important role in maximizing the extraction yield (Vázquez *et al*. 2008). Furthermore, various non-conventional or innovative extraction methods have been effectively advanced and applied to optimize the plant materials' bioactive compounds' extraction, such as ultrasound-assisted extraction (UAE) and microwave-assisted extraction (MAE) (Xu *et al*. 2017).

Physicochemical Characterization

FTIR spectroscopy

The FTIR spectra of the TME and TAE were recorded in the region of 4000 cm^{-1} to 400 cm^{-1}, as shown in Fig. 1, and all the absorption bands are presented in Table 1. The absorption peaks obtained were similar to that of Aleppo pine tannin (Saad *et al*. 2014) and catechin standard (Kassim *et al*. 2011). Peaks positioned at 3411 cm^{-1} and 3396 cm^{-1} (TME and TAE, respectively) were attributed to stretching vibrations of OH

bonds (Ping *et al*. 2012a). The IR bands located at 2925 cm^{-1} to 2924 cm^{-1} and 2861 cm^{-1} to 2852 cm^{-1} for TME and TAE correspond to CH_2 and CH vibrations of an aliphatic hydrocarbon, respectively (Lee and Lan 2006; Ping *et al*. 2012b). Absorption bands at 1610 cm^{-1} and 1611 cm^{-1}, 1522 cm^{-1} and 1521 cm^{-1}, and 1450 cm^{-1} and 1444 cm^{-1} (TME and TAE, respectively) denote stretching vibrations of aromatic rings. Moreover, IR bands observed at 1050 cm^{-1} to 1261 cm^{-1} and 1068 cm^{-1} to 1284 cm^{-1} (TME and TAE, respectively) correspond to symmetrical stretching vibration of C-O-C, (Lee and Lan 2006). The IR peaks at 1378 cm^{-1} and 1375 cm^{-1} TME and TAE were attributed to the O-H stretching vibrations of phenolic groups and C-H deformations of aliphatic groups, respectively (Chupin *et al*. 2013).

However, there was a slight shifting of peaks among the tannin samples compared to the standard, which could be attributed to the differences in purity and crystallinity of the samples.

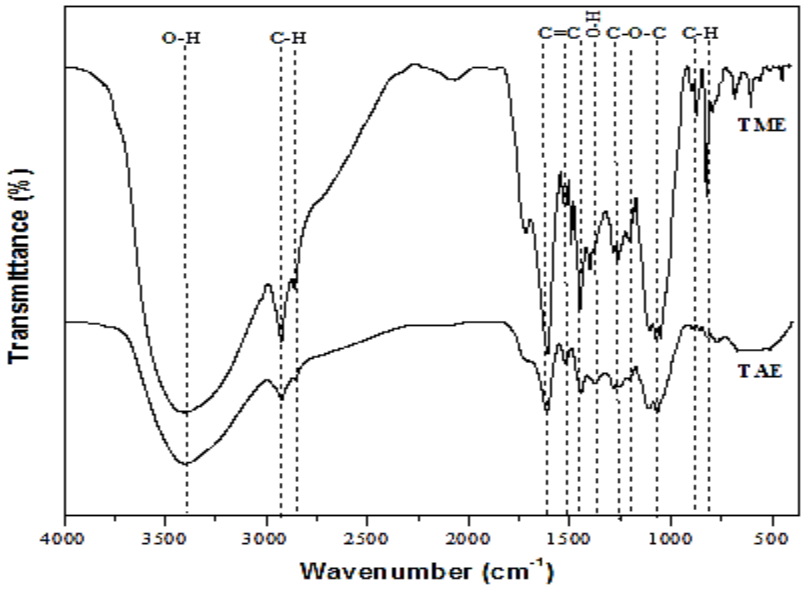

Fig. 1. FTIR spectra of TME and TAE

Table 1. Assignment of FTIR Spectra of TME and TAE

Assignment	Wavenumber (cm^{-1})	
	TME	TAE
OH stretching vibration	3411	3396
CH_2 vibration of aliphatic hydrocarbon	2925	2924
CH vibration of aliphatic hydrocarbon	2861	2852
C=C aromatic ring stretching vibration	1610,1522,1450	1611,1521,1444
OH stretching vibration	1378	1375
C-O-C symmetric stretching vibration	1261,1104,1050	1284,1111,1068

NMR spectroscopy

The ^1H NMR spectra of TME and TAE were deduced according to a study described by Arbenz and Avérous (2014). Figure 2 depicts typical signals of the spectra and shows distinct regions: 8.0 ppm to 6.0 ppm, attributed to the aromatic protons; 5.2 ppm to 2.6 ppm, representing methoxy protons; and 1.4 ppm to 0.5 ppm, symbolizing aliphatic protons.

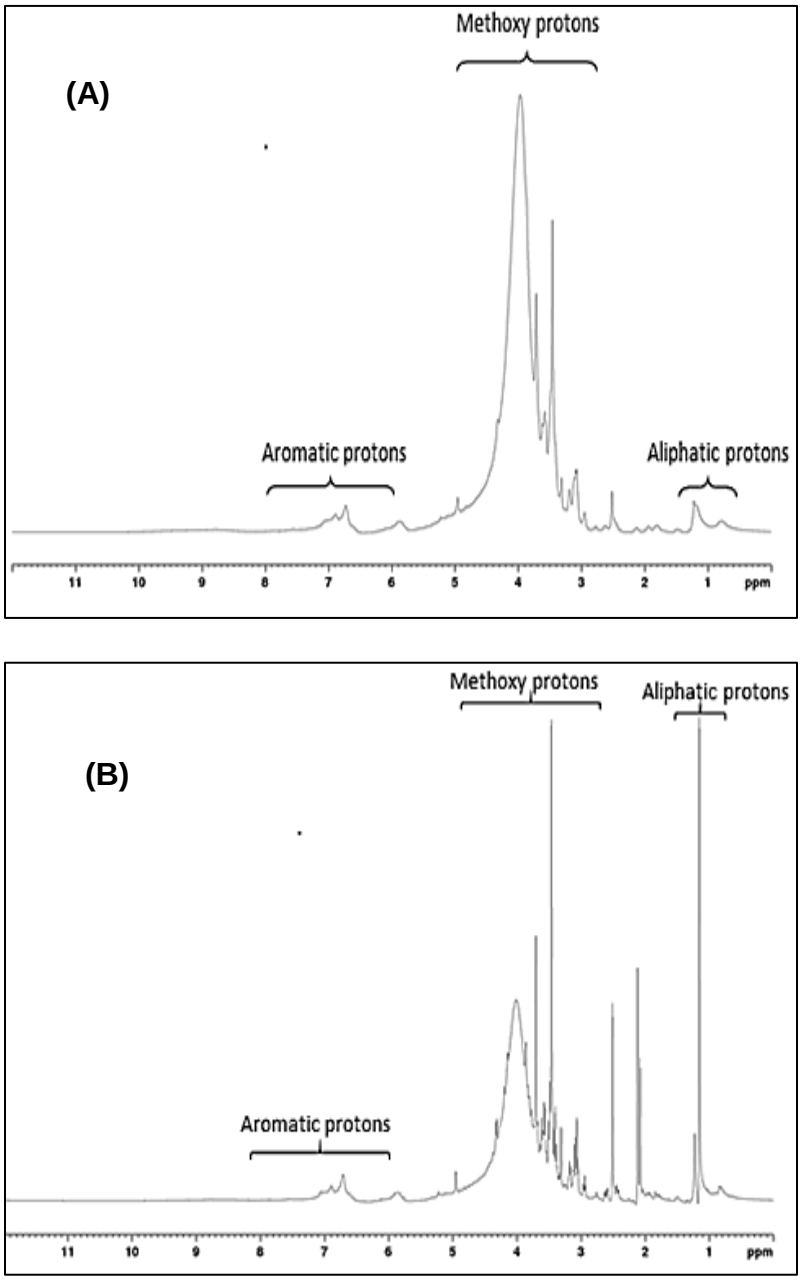

Fig. 2. ^{1}H NMR spectra of (A) TME and (B) TAE in DMSO

The ^{13}C NMR spectra depicted in Fig. 3 show peaks similar to those of Aleppo pine tannin extract (Saad *et al*. 2014) and grape pomace tannin extract (Ping *et al*. 2011). The tannin spectra exhibited the conventional signals of prodelphinidin (PD) and procyanidin (PC) entities, with majority of PC units. The peaks between 115 ppm and 120 ppm signify C2′, C6′, and C5′ carbons of procyanidin entities. The NMR signals present from 142 ppm to 145 ppm correspond to C3′ and C4′ carbons of procyanidin entities. It can be deduced that the NMR peaks of C5, C7, and C8a carbons in procyanidin entities lie between 150 ppm and 160 ppm. Prodelphinidin entities were identified from the chemical shift of C4 positioned at 130.8 ppm, which overlaps with the signal representing C1' carbon. Signals present between 90 ppm and 110 ppm were denoted as C8, C6, C6′, and C2′ of procyanidin entities. The C4 extension units

demonstrated a broad peak at 36.6 ppm, but terminal C4 showed a distinctive signal at 29.4 ppm. Presence of carbohydrates in both extracts was represented by the peaks between 60 ppm and 85 ppm (Fu *et al*. 2007; Zhang and Lin 2008; Zhang *et al*. 2010).

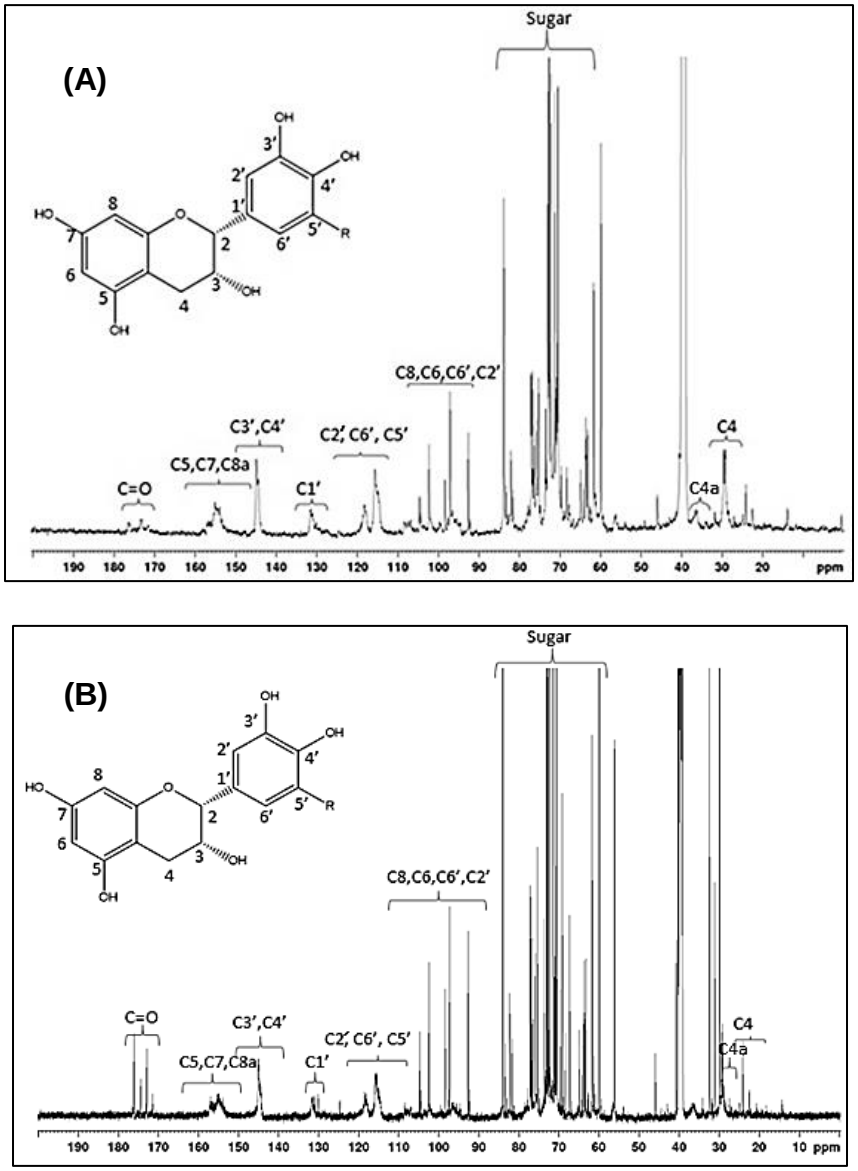

Fig. 3. ^{13}C NMR spectra of (A) TME and (B) TAE in DMSO.

TGA

To describe the thermal stability of both tannin samples, thermal degradation analysis was conducted. As presented in Fig. 4, thermogravimetric (TG) curves indicate loss of weight for the TME and TAE samples in relation to degradation temperature, while the rate of weight loss is shown through derivative thermogravimetric (DTG) analysis. At almost 30 °C, the first degradation of tannin was observed due to the loss of H_2O, CO, CO_2, and other unstable products (Sun *et al*. 2001; Hussin *et al*. 2013). Subsequent degradations observed at approximately 152 °C (TME) and 148 °C (TAE) indicated the loss of hemicellulose attached to tannins (García *et al*. 2009), and those at 208 °C (TME) and 204 °C (TAE) were attributed to the decomposition of tannin

structures (Saad *et al*. 2014). The maximum rate of weight loss (DTG_{max}) was at 300 °C for TME, which was greater than the 265 °C obtained for TAE. This is due to the different stabilities of the extracts. Approximately 30.98% of the TME and 29.71% of the TAE remained at 900 °C. Moreover, it was evident that both the tamarind shell tannin extracts (TSTE) were more thermally stable than Tunisian Aleppo pine tannins (179 °C) (Saad *et al*. 2014) and radiata pine tannins (150 °C) (Luo *et al*. 2010).

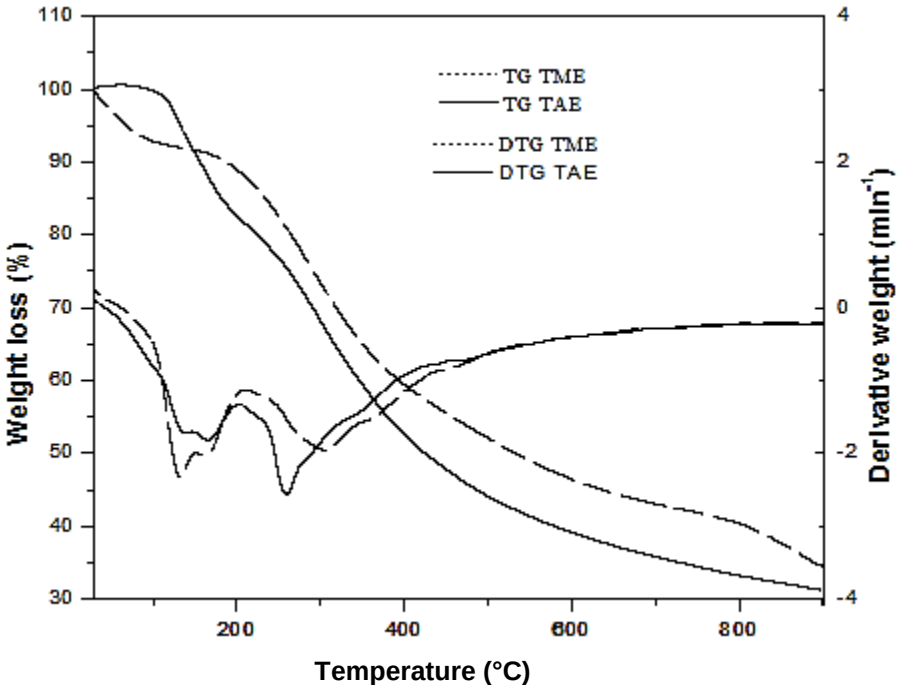

Fig. 4. TG and derivative thermogravimetric DTG curves of TME and TAE

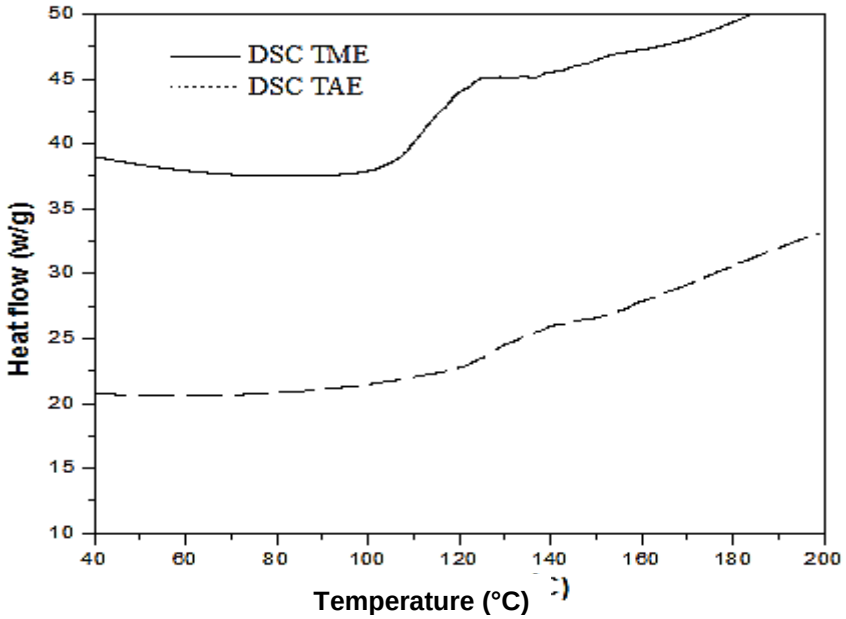

Fig. 5. DSC of TME and TAE

Differential scanning chromatography

DSC is the most commonly known method for determining the glass transition temperature of synthetic and natural polymers and mostly to study the thermal behavior of a polymer, despite the complex structure of tannin. TME showed a lower T_g value than that of TAE (T_g TAE: 127.26 °C > T_g TME: 112.39 °C) as shown in Fig. 5, suggesting that TME has a less complex structure, and its bonds can be easily broken to form smaller structures compared to TAE. Hence, to obtain the T_g value of complex structure, polymers need additional energy, which leads to a high value of T_g (Hussin *et al*. 2018).

Phytochemical Assays

Total phenolic content (TPC)

Table 2 outlines the varying values of TPC for each solvent with dissimilar polarity index. Folin-Ciocalteu assay method of the different types of solvents was used to compare the presences of extracted phenolic compounds. The Folin-Ciocalteu reagent reduction changes its solution colour, into blue by phenolic ions (Prior *et al*. 2005). The extract contains more phenolic compounds when the complex reduction increases. Thus, the absorbance would be higher, and the colour would be darker (Arbianti *et al*. 2007). The results showed that TME contained the greatest TPC, followed by TAE. Earlier studies have determined *Tamarindus indica* L, 0.44 ± 0.01 mg/ml GAE (Povichit *et al*. 2010). *Tamarindus indica* L, 2.82 g / kg GAE (Sudjaroen *et al*. 2005), and Tunisian Aleppo pine barks tannin content, which was 64.5 mg g^{-1} GAE ± 5.3 mg g^{-1} GAE (Saad *et al*. 2014).

Table 2. Total Phenolic, Total Flavonoid, and Total Tannin Contents

Extract	Total Phenolic Content (GAE mg g^{-1})	Total Flavonoid Content (CE mg g^{-1})	Total Tannin Content (%)
TME	68.67 ± 0.26	57.38 ± 0.2	86.66
TAE	53.82 ± 0.13	49.50 ± 0.5	73.33

Total flavonoid content (TFC)

Evaluation of the TFC in a plant material pertaining to a colorimetric determination reaction with $AlCl_3$ is a well-known method (Zhishen *et al*. 1999). The hydroxyl group of flavonoids and flavanols forms stable acid complexes with aluminium chloride (Chang *et al*. 2002; Mohy-ud-Din *et al*. 2009). Table 2 presents the catechin equivalent (CE) of different extraction solvents. Clearly, TME had the greatest CE value of 57.38 mg g^{-1}. This result showed that extraction of flavonoids from tamarind shells using methanol was more efficient compared to acetone extraction. Meanwhile, a previous study reported that *Uncaria gambir* had a CE of 93.31 mg g^{-1} CE (Kassim *et al*. 2011).

Total tannin content (TTC)

TTC determination aims to investigate the percentage of tannins in tamarind shell extract that reacts with formaldehyde, forming phenol-formaldehyde resin (Garro-Galvez *et al*. 1996). Table 2 depicts the content of Stiasny precipitate in terms of percentage, with TME offering the most significant percentage value of 86.7%. Tamarind shell tannins extracted with methanol resulted in a greater Stiasny precipitate compared to acetone extract. According to previous studies, *Tamarindus indica* L had a TTC of 39%

(Sinchaiyakit *et al.* 2011), *Tamarindus indica* 77% (Sudjaroen *et al*. 2005), Tunisian Aleppo 82.5% (Saad *et al*. 2014), and Quebracho had a TTC of 88.3% (Gerengi and Sahin 2012).

Meanwhile, the reasons for the variability in total phenolic, flavonoid, and tannin contents appear to be the geographical growth sites of the plant and the natures of the species (Yesil-Celiktas *et al*. 2009). Varying the parameters of extraction, solvent medium, and extraction technique could also be the cause of this variability (Vázquez *et al*. 2008).

Rust Conversion Studies

FTIR analysis of rust

Figure 6 depicts rust standard FTIR spectra of goethite (α-FeOOH), lepidocrocite (γ-FeOOH), and magnetite (Fe_3O_4). The H_2O absorption in almost all samples was present at approximately 1642 cm^{-1}, 1619 cm^{-1}, and 1641 cm^{-1}. The FTIR spectrum of lepidocrocite displayed absorption bands at 1153 cm^{-1} (medium), 1021 cm^{-1} (strong), 889 cm^{-1} (medium), 749 cm^{-1} (medium), and 472 cm^{-1} (strong). Hence, the 1021 cm^{-1} IR band was the strongest and can be considered as lepidocrocite's major band. The lepidocrocite spectrum containing bands at 1150 cm^{-1}, 1020 cm^{-1}, and 750 cm^{-1} gave evidence of a highly crystalline state (Nasrazadani 1997).

The FTIR spectrum of the goethite had its peaks at 1033 cm^{-1} (strong), 904 cm^{-1} (strong), 798 cm^{-1} (strong), 612 cm^{-1} (weak), and 532 cm^{-1} (weak). Very strong peaks were observed at 904 cm^{-1} and 798 cm^{-1}, which are considered as goethite's main typical peaks. Goethite had IR absorption peaks in its crystalline state at approximately 1644 cm^{-1}, 1386 cm^{-1}, 890 cm^{-1}, 769 cm^{-1}, and 650 cm^{-1}. The FTIR spectrum of magnetite presented a strong peak at 569 cm^{-1} and a less intense peak at 444 cm^{-1} (weak). Detected peaks which corroborate these results establish that magnetite has two major distinctive peaks at 568 cm^{-1} and 473 cm^{-1} (Gust 1991; Nasrazadani 1997).

Figure 6 also depicts the FTIR spectrum of salt-spray-generated rust. It was revealed that γ-FeOOH, α-FeOOH, and Fe_3O_4 were the main steel rust products.

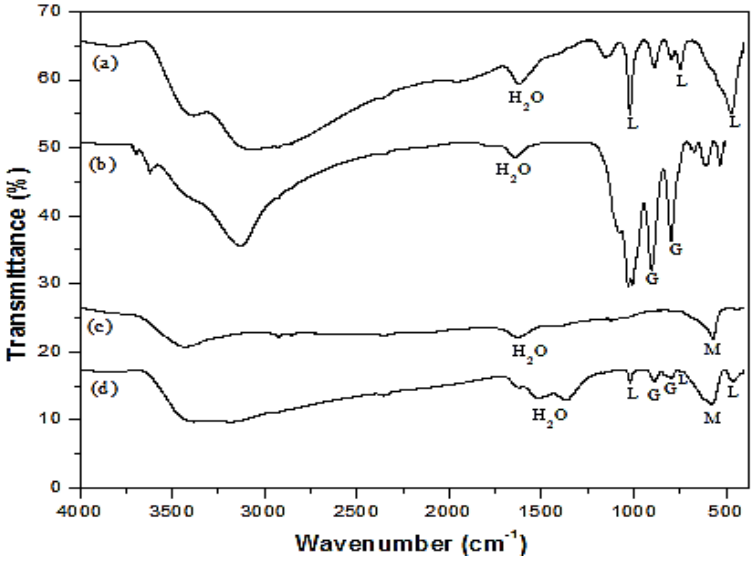

Fig. 6. FTIR spectra of rust standards; (a) lepidocrocite, (b) goethite, (c) magnetite, and (d) salt-spray-generated rust

Previous studies revealed that at typical ambient conditions, γ-FeOOH, α-FeOOH, and Fe_3O_4 are the main components of any rust system pertaining to a steel surface (Gust 1991; Favre and Landolt 1993). It was also noted that the method of preparation determines the rust components (Rahim *et al*. 2011). These peaks affirmed the resemblance of similar strengths of absorption with the standard but with a slightly dissimilar frequency, which might be due to the purity and amorphous nature of the samples (Dahon *et al*. 2018).

The effect of concentration

Varied concentrations were employed to evaluate the tamarind shell extract effect on rust transformation. The following formula (Eq. 1) was adopted for the calculation of the rate of transformation of rust in terms of percentage (*RT %*) (Dahon *et al*. 2018),

$$RT\,\% = \frac{I_0 - I_i}{I_0} \times 100 \quad (1)$$

where I_0 is the control peak intensity of lepidocrocite, goethite, and magnetite, respectively, before treatment, and I_i is the sample peak intensity after treatment.

The FTIR spectra of various concentrations (1 wt% to 7 wt%) of TME and TAE rust powder treatments are shown in Fig. 7, which depicts the IR absorption data of rust treated with 1 wt% to 7 wt% TME and TAE upon 24 h treatment.

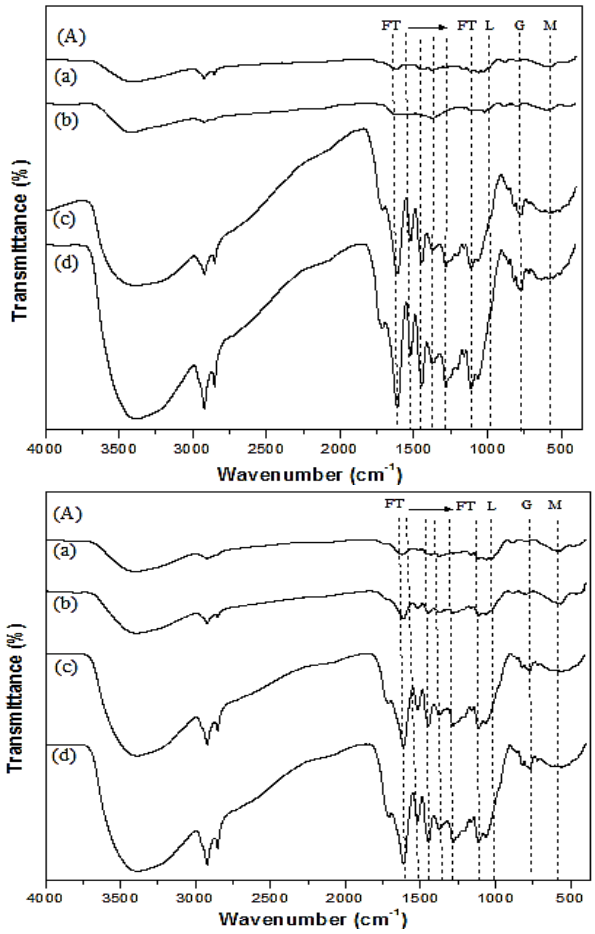

Fig. 7. FTIR spectra of rust after 24 h treatment at (a) 1 wt%, (b) 3 wt%, (c) 5 wt%, and (d) 7 wt% of (A) TME and (B) TAE

It was observed that the strengths of each of the rust's basic constituents were reduced starting from 1 wt% at pH 5 upon 24 h of immersion. The strength of lepidocrocite's main peak situated at 1019 cm^{-1} disappeared completely on the addition of 5 wt% to 7 wt% of both TME and TAE. Other peaks of lepidocrocite at 745 cm^{-1} and 462 cm^{-1} also completely disappeared when adding 5 wt% to 7 wt% of TME and TAE, which could be due to the complexation reaction between tannin and iron. The goethite peaks located at 888 cm^{-1} disappeared completely with the addition of 5 wt% to 7 wt% of, each, TME and TAE, while the peak at 796 cm^{-1} slightly reduced. Magnetite's major rust peak situated at 578 cm^{-1} became broader, and the frequency was shifted from 578 cm^{-1} to 641 cm^{-1} in the case of TME and to 593 cm^{-1} for TAE at a concentration of 7 wt%. However, the percentage of the rust transformation (RT) was up to 92.5% for TME and 91.7% for TAE.

Thus, the trend of these results was similar to that of *Uncaria gambir* (Dahon *et al*. 2018). New peaks in the range of 1611 cm^{-1} to 1113 cm^{-1} were observed for both the TME and TAE, which denoted the formation of ferric tannate (Nasrazadani 1997). Based on the acquired spectra, 7 wt% of TME and TAE at the level of the study turns out to be the optimum concentration for rust powder treatment. Meanwhile, the effects of other concentrations on rust treatment presented a significant percentage of rust transformation, with 1 wt% of TME and TAE demonstrating 63.3% and 50.4% RT, while 3 wt% TME and TAE showed 68.3% and 63.2% RT, respectively. However, 5 wt% TME showed 91.6%, and TAE showed 90.8%.

The effect of pH

For pH adjustment, 0.1 M HCl and NaOH were designated to study their effects on rust transformation, utilizing TME and TAE at optimum concentration (7 wt%), subjected to a 24-h immersion. Figure 8 depicts the spectra of rust with varied pH values (1, 3, 5, 7, 9, and 11) upon the addition into the treatment solution. As observed from the spectra obtained, varying pH treatments offered varied shifting of peaks and a notable reduction in intensities.

However, magnetite's major peak located at 578 cm^{-1} shifted to 631 cm^{-1} and 626 cm^{-1} upon treatment with TME and TAE at pH 3, reaching RT up to 95% and 93.3%, respectively, which could be attributed to complexation reactions of tannin and iron at lower pH values.

Furthermore, few changes were observed with goethite's peak. Meanwhile, the percentages of rust transformation related to other varying pH values were also determined: At a pH of 1, the RT of TME and TAE was 90.0% and 88.3%, respectively. At a pH of 5, TME had an RT of 92.5%, and TAE had an RT of 91.7%. At a pH of 7, it was 91.5% for TME and 90.7% for TAE. At a pH of 9, it was 84.3% for TME and 83.4% for TAE. At a pH of 11, it was 78.3% and 76.7% for TME and TAE, respectively. Thus, the lower RT values at higher pH values might be because, at low pH, solutions with the excess of H^+ will react and dissolve rust better than high pH solutions with an excess of OH^-. Therefore, it suggests that a pH of 3 yielded the optimum pH for rust transformation.

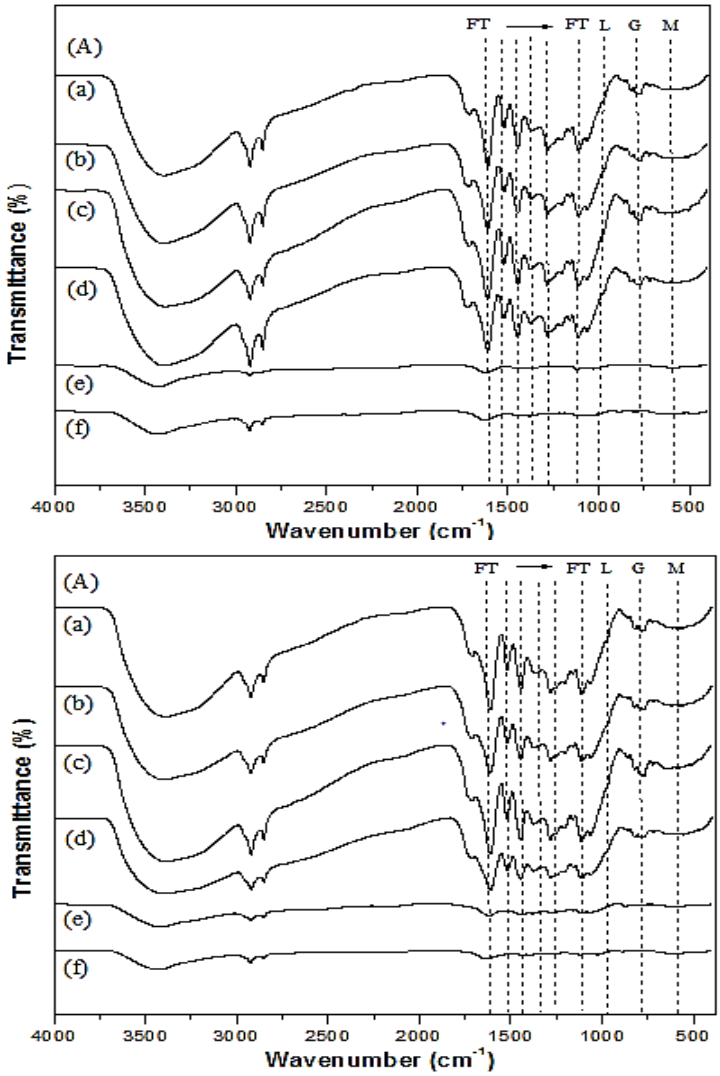

Fig. 8. FTIR spectra of rust after 24 h treatment at (a) pH 1, (b) pH 3, (c) pH 5, (d) pH 7, (e) pH 9, and (f) pH 11, with 7 wt% of (A) TME and (B) TAE

Effect of reaction time

Reaction time periods designated in this study were 1 d, 3 d, 5 d, 7 d, and 14 d. Figure 9 depicts the spectra of rust samples upon treatment with 7 wt% TME and TAE at a pH of 3 for various immersion time intervals. The spectra showed obvious changes in the intensity of rust constituents as the time of immersion was increased. This might be due to the formation of ferric tannate. The magnetite peak located at 578 cm^{-1} shifted to 648 cm^{-1} for TME and 642 cm^{-1} for TAE. Up to 95.8% of rust transformation was accomplished after 3 d upon treatment with TME, with up to 94.8% upon 5 d of treatment using TAE. Furthermore, the peaks remained the same throughout the entire time duration, suggesting the effect of saturation by the reaction solution. Peaks appearing from 1611 cm^{-1} to 1113 cm^{-1} were attributed to the formation of ferric tannate (Nasrazadani 1997). These findings suggests that the optimum reaction time was 3 days for TME and 5 days for TAE at the level of our study.

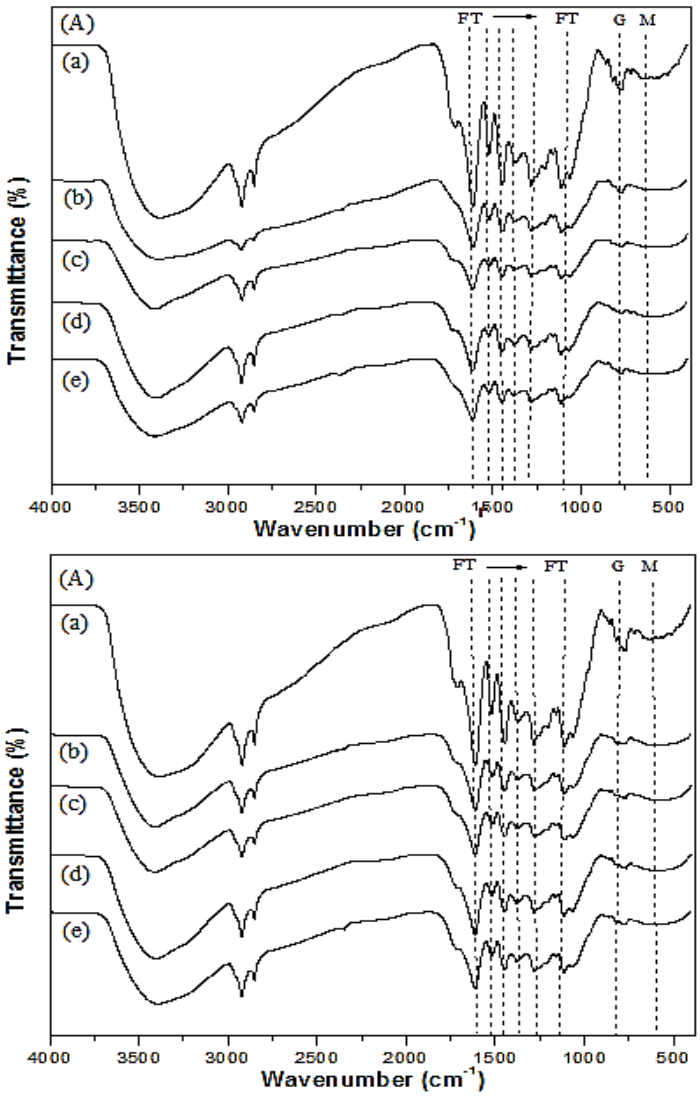

Fig. 9. FTIR spectra of rust upon treatment with 7 wt% of (A) TME and (B) TAE for (a) 1 d, (b) 3 d, (c) 5 d, (d) 7 d, and (e) 14 d of contact time

FTIR signals of ferric tannate

The absorption peaks attributed to the ferric tannate region were similar to that of ferric tannate reported by Zhang *et al.* (2015). The TME and TAE ferric tannate composites are presented. Two broad absorption bands in the range of 3437 cm^{-1} (TME) and 3429 cm^{-1} (TAE) indicated the presence of the phenolic hydroxyl group, and the peaks at 1356 cm^{-1} (TME) and 1374 cm^{-1} (TAE) show characteristic bending vibration of O-C of the phenolic hydroxyl group. The absorption bands at 1435 cm^{-1} (TME) and 1444 cm^{-1} (TAE) in the region of the ferric tannate complex are attributed to C=O of benzoic acid vibration. This occurrence can be described by the redox and the chelation reaction of Fe^{3+} with the phenolic hydroxyl group, which effects in concurrence of Fe^{3+} and Fe^{2+} in ferric tannate. The interaction of Fe^{3+} and the phenolic hydroxyl group affects the bond stretching vibration of O-C in the region of the ferric tannate composite. The anion of oxygen was formed as a result of the arrangement process of Fe^{3+} with the phenolic hydroxyl group.

Mechanism of rust transformation

The mechanism of rust transformation was deduced by Rahim *et al*. (2011) that tannin complexation reaction with iron, as presented in Fig. 10, occurring based on three possibilities: First, the tannins can complex with Fe^{2+} ions to form Fe^{2+}-tannate, which oxidizes easily into Fe^{3+}-tannates in reaction with oxygen. Second, Fe^{3+} ions can directly react with tannin to form Fe^{3+}-tannates. Third, reduction of Fe^{3+} oxides to Fe^{2+} ions by tannin and complexation with tannin to form Fe^{2+}-tannate and in the presence of oxygen it oxidizes into Fe^{3+}-tannate.

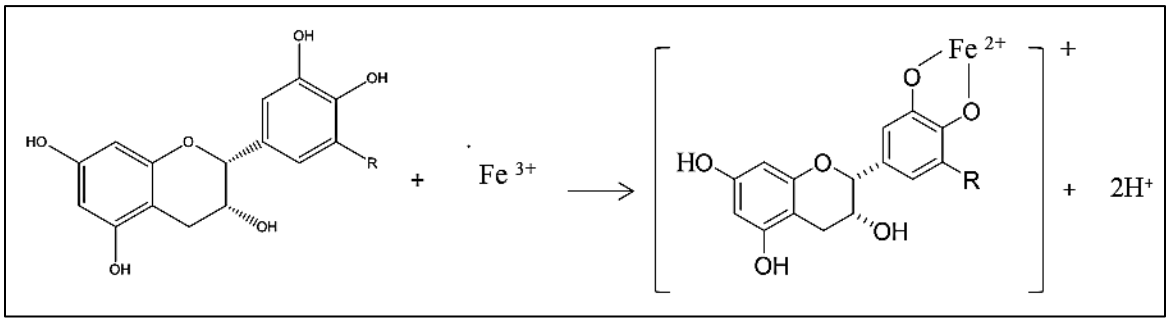

Fig. 10. Schematic of rust transformation mechanism of tannin-iron complex (Zhang *et al.* 2015)

CONCLUSIONS

1. Colorimetric assays revealed that tamarind shells are rich in phytochemical compounds.
2. The results of FTIR and ^{13}C NMR analyses confirmed the presence of tannins. Thermogravimetric analysis presented the thermal stability of tamarind shell tannin extracts.
3. The methanol extract of tamarind shell (TME) showed better performance of rust transformation, reaching up to 95.8%, while the aqueous acetone extract of tamarind shell (TAE) achieved 94.8% of rust transformation (RT). This result is due to the greater polarity and greater solubility in methanol.
4. The appearance of new peaks indicated the formation of ferric tannate. The rust transformation was in the order of lepidocrocite > magnetite > goethite, as previously shown.

ACKNOWLEDGMENTS

The authors acknowledge Hassan Usman Katsina Polytechnic for the PhD sponsorship and Universiti Sains Malaysia for providing USM short term Grant – 304/PKIMIA/6315100. Tuan Sherwyn Hamidon extends his gratitude to Universiti Sains Malaysia for the financial assistance through the USM Graduate Assistant Scheme.

REFERENCES CITED

Arbenz, A., and Avérous, L. (2014). "Synthesis and characterization of fully biobased aromatic polyols–oxybutylation of condensed tannins towards new macromolecular architectures," *RSC Advances* 4(106), 61564-61572. DOI: 10.1039/C4RA10691A

Arbianti, R., Utami, T. S., Kurmana, A., and Sinaga, A. (2007). "Comparison of antioxidant activity and total phenolic content of *Dillenia indica* leaves extracts obtained using various techniques," in: *14th Regional Symposium on Chemical Engineering*, Yogyakarta, Indonesia.

ASTM (1973). "Standard method of salt spray (fog) testing," American Society of Testing Materials. ASTM B 117-73; 1-8

Balasundram, N., Sundram, K., and Samman, S. (2006). "Phenolic compounds in plants and agri-industrial by-products: Antioxidant activity, occurrence, and potential uses," *Food Chemistry* 99(1), 191-203. DOI: 10.1016/j.foodchem.2005.07.042

Barrero, C. A., Ocampo, L. M., and Arroyave, C. E. (2001). "Possible improvements in the action of some rust converters," *Corrosion Science* 43(6), 1003-1018. DOI: 10.1016/S0010-938X(00)00139-6

Chang, C. C., Yang, M. H., Wen, H. M., and Chern, J. C. (2002). "Estimation of total flavonoid content in propolis by two complementary colorimetric methods," *Journal of Food and Drug Analysis* 10, 178-182.

Chupin, L., Motillon, C., Charrier-El Bouhtoury, F., Pizzi, A., and Charrier, B. (2013). "Characterisation of maritime pine (*Pinus pinaster*) bark tannins extracted under different conditions by spectroscopic methods, FTIR and HPLC," *Industrial Crops and Products* 49, 897-903. DOI: 10.1016/j.indcrop.2013.06.045

Dahon, N. H., Kassim, M. J., Razali, N. N., Yuslee, E. M. F. M., Nasrullah, A. A., and Basri, N. F. (2018). "FTIR analysis on phase transformation of rust in the presence of gambir," *Journal of Global Scientific Research* 1, 54-62.

Favre, M., and Landolt, D. (1993). "The influence of gallic acid on the reduction of rust on painted steel surfaces," *Corrosion Science* 34(9), 1481-1494. DOI: 10.1016/0010-938X(93)90243-A

Feliu, S., Galván, J. C., Feliu, Jr., S., Bastidas, J. M., Simancas, J., Morcillo, M., and Almeida, E. M. (1993). "An electrochemical impedance study of the behaviour of some pretreatments applied to rusted steel surfaces," *Corrosion Science* 35(5-8) 1351-1358. DOI: 10.1016/0010-938X(93)90357-M

Fu, C., Loo, A. E. K., Chia, F. P. P., and Huang, D. (2007). "Oligomeric proanthocyanidins from mangosteen pericarps," *Journal of Agricultural and Food Chemistry* 55(19), 7689-7694. DOI: 10.1021/jf071166n

García, A., Toledano, A., Serrano, L., Egüés, I., González, M., Marín, F., and Labidi, J. (2009). "Characterization of lignins obtained by selective precipitation," *Separation and Purification Technology* 68(2), 193-198. DOI: 10.1016/j.seppur.2009.05.001

Garro-Galvez, J. M., Fechtal, M., and Riedl, B. (1996). "Gallic acid as a model of tannins in condensation with formaldehyde," *Thermochimica Acta* 274, 149-163. DOI: 10.1016/0040-6031(95)02630-4

Gerengi, H., and Sahin, H. I. (2012). "*Schinopsis lorentzii* extract as a green corrosion inhibitor for low carbon steel in 1 M HCl solution," *Industrial & Engineering Chemistry Research* 51(2), 780-787. DOI: 10.1021/ie201776q

Gust, J., and Suwalski, J. (1994). "Use of Mossbauer spectroscopy to study reaction products of polyphenols and iron compounds," *Corrosion* 50(5), 355-365.

Gust, J. (1991). "Application of infrared spectroscopy for investigation of rust phase component conversion by agents containing oak tannin and phosphoric acid," *Corrosion* 47(6), 453-457. DOI: 10.5006/1.3585278

Gust, J., and Bobrowicz, J. (1993). "Sealing and anti-corrosive action of tannin rust converters," *Corrosion* 49(1), 24-30. DOI: 10.5006/1.3316030

Haslam, E. (1989). *Plant Polyphenols: Vegetable Tannins Revisited*, Cambridge University Press, Cambridge, UK.

Hussin, M. H., Rahim, A. A., Ibrahim, M. N. M., and Brosse, N. (2013). "Physicochemical characterization of alkaline and ethanol organosolv lignins from oil palm (*Elaeis guineensis*) fronds as phenol substitutes for green material applications," *Industrial Crops and Products* 49, 23-32. DOI: 10.1016/j.indcrop.2013.04.030

Hussin, M. H., Samad, N. A., Latif, N. H. A., Rozuli, N. A., Yusoff, S. B., Gambier, F., and Brosse, N. (2018). "Production of oil palm (*Elaeis guineensis*) fronds lignin-derived non-toxic aldehyde for eco-friendly wood adhesive," *International Journal of Biological Macromolecules* 113, 1266-1272. DOI: 10.1016/j.ijbiomac.2018.03.048

Kassim, M. J., Hussin, M. H., Achmad, A., Dahon, N. H., Suan, T. K., and Hamdan, H. S. (2011). "Determination of total phenol, condensed tannin and flavonoid contents and antioxidant activity of *Uncaria gambir* extracts," *Indonesian Journal of Pharmacy* 22(1), 50-59. DOI: 10.14499/indonesianjpharm0iss0pp50-59

Khanbabaee, K., and van Ree, T. (2001). "Tannins: Classification and definition," *National Product Reports* 18(6), 641-649. DOI: 10.1039/B101061L

Lee, W.-J., and Lan, W.-C. (2006). "Properties of resorcinol–tannin–formaldehyde copolymer resins prepared from the bark extracts of Taiwan acacia and China fir," *Bioresource Technology* 97(2), 257-264. DOI: 10.1016/j.biortech.2005.02.009

Lokeswari, N., and Sujatha, P. (2011). "Isolation of tannins from *Caesalpinia coriaria* and effect of physical parameters," *International Research Journal of Pharmacy* 2(2), 146-152. http://www.irjponline.com

Luengthanaphol, S., Mongkholkhajornsilp, D., Douglas, S., Douglas, P. L., Pengsopa, L. I., and Pongamphai, S. (2004). "Extraction of antioxidants from sweet Thai tamarind seed coat—preliminary experiments," *Journal of Food Engineering* 63(3), 247-252.

Luo, C., Grigsby, W., Edmonds, N., Easteal, A., and Al-Hakkak, J. (2010). "Synthesis, characterization, and thermal behaviors of tannin stearates prepared from quebracho and pine bark extracts," *Journal of Applied Polymer Science* 117(1), 352-360. DOI: 10.1002/app.31545

Matamala, G., Smeltzer, W., and Droguett, G. (2000). "Comparison of steel anticorrosive protection formulated with natural tannins extracted from acacia and from pine bark," *Corrosion Science* 42(8), 1351-1362. DOI: 10.1016/S0010-938X(99)00137-7

Mabrour, J., Akssira, M., Azzi, M., Zertoubi, M., Saib, N., Messaoudi, A., Albizane, A., and Tahiri, S. (2004). "Effect of vegetal tannin on anodic copper dissolution in chloride solutions," *Corrosion Science* 46(8), 1833-1847.

McDonald, S., Prenzler, P. D., Antolovich, M., and Robards, K. (2001). "Phenolic content and antioxidant activity of olive extracts," *Food Chemistry* 73(1), 73-84. DOI: 10.1016/S0308-8146(00)00288-0

Mercola. (2015). "What is tamarind good for?," (http://foodfacts.mercola.com/tamarind.html), accessed 7 December 2016.

Mohy-ud-Din, A., Khan, Z.-u.-D., Ahmad, M., Kashmiri, M. A., Yasmin, S., and Mazhar, H. (2009). "Chemotaxonomic significance of flavonoids in the *Solanum nigrum* complex," *Journal of the Chilean Chemical Society* 54(4), 486-490. DOI: 10.4067/S0717-97072009000400037

Nasrazadani, S. (1997). "The application of infrared spectroscopy to a study of phosphoric and tannic acids interactions with magnetite (Fe_3O_4), goethite (α-FEOOH) and lepidocrocite (γ-FeOOH)," *Corrosion Science* 39(10-11), 1845-1859. DOI: 10.1016/S0010-938X(97)00060-7

Pereyra, A. M., Herrera, L. K., Echeverría, F. E., Castaño, J. G., and Giudice, C. A. (2006). "Renewable rust inhibitors," *European Coatings Journal* 3, 24.

Povichit, N., Phrutivorapongkul, A., Suttajit, M., Chaiyasut, C., and Leelapornpisid, P. (2010). "Phenolic content and in vitro inhibitory effects on oxidation and protein glycation of some Thai medicinal plants," *Pak. J. Pharm. Sci*. 23(4), 403-408.

Ping, L., Pizzi, A., Guo, Z. D., and Brosse, N. (2011). "Condensed tannins extraction from grape pomace: Characterization and utilization as wood adhesives for wood particleboard," *Industrial Crops and Products* 34(1), 907-914. DOI: 10.1016/j.indcrop.2011.02.009

Ping, L., Gambier, F., Pizzi, A., Guo, Z. D., and Brosse, N. (2012a). "Wood adhesives from agricultural by-products: Lignins and tannins for the elaboration of particleboards," *Cellulose Chemistry and Technology* 46(7), 457-462.

Ping, L., Pizzi, A., Guo, Z. D., and Brosse, N. (2012b). "Condensed tannins from grape pomace: Characterization by FTIR and MALDI TOF and production of environment friendly wood adhesive," *Industrial Crops and Products* 40, 13-20. DOI: 10.1016/j.indcrop.2012.02.039

Prior, R. L., Wu, X., and Schaich, K. (2005). "Standardized methods for the determination of antioxidant capacity and phenolics in foods and dietary supplements," *Journal of Agricultural and Food Chemistry* 53(10), 4290-4302. DOI: 10.1021/jf0502698

Rahim, A. A., Kassim, M. J., Rocca, E., and Steinmetz, J. (2011). "Mangrove (*Rhizophora apiculata*) tannins: An eco-friendly rust converter," *Corrosion Engineering, Science and Technology* 46(4), 425-431. DOI: 10.1179/174327809X457003

Ross, T. K., and Francis, R. A. (1978). "The treatment of rusted steel with mimosa tannin," *Corrosion Science* 18(4), 351-361. DOI: 10.1016/S0010-938X(78)80049-3

Saad, H., Khoukh, A., Ayed, N., Charrier, B., and Charrier-El Bouhtoury, F. (2014). "Characterization of Tunisian Aleppo pine tannins for a potential use in wood adhesive formulation," *Industrial Crops and Products* 61, 517-525. DOI: 10.1016/j.indcrop.2014.07.035

Sinchaiyakit, P., Ezure, Y., Sriprang, S., Pongbangpho, S., Povichit, N., and Suttajit, M. (2011). "Tannins of tamarind seed husk: preparation, structural characterization, and antioxidant activities," *Natural Product Communications* 6(6), 1934578X1100600619.

Sudjaroen, Y., Haubner, R., Würtele, G., Hull, W. E., Erben, G., Spiegelhalder, B., Changbumrung, S., Bartsch, H., and Owen, R. W. (2005). "Isolation and structure elucidation of phenolic antioxidants from tamarind (*Tamarindus indica* L.) seeds and pericarp," *Food and Chemical Toxicology* 43(11), 1673-1682.

Sun, R., Lu, Q., and Sun, X. F. (2001). "Physico-chemical and thermal characterization of lignins from *Caligonum monogoliacum* and *Tamarix* spp.," *Polymer Degradation and Stability* 72(2), 229-238. DOI: 10.1016/S0141-3910(01)00023-4

Vázquez, G., Fontenla, E., Santos, J., Freire, M. S., González-Álvarez, J., and Antorrena, G. (2008). "Antioxidant activity and phenolic content of chestnut (*Castanea sativa*) shell and eucalyptus (*Eucalyptus globulus*) bark extracts," *Industrial Crops and Products* 28(3), 279-285. DOI: 10.1016/j.indcrop.2008.03.003

Xu, D.-P., Li, Y., Meng, X., Zhou, T., Zhou, Y., Zheng, J., Zhang, J.-J., and Li, H.-B. (2017). "Natural antioxidants in foods and medicinal plants: Extraction, assessment and resources," *International Journal of Molecular Sciences* 18(1), 96. DOI: 10.3390/ijms18010096

Yahya, S., Shah, A. M., Rahim, A. A., Aziz, N. H. A., and Roslan, R. (2008). "Phase transformation of rust in the presence of various tannins," *Journal of Physical Science* 19(1), 31-41.

Yazaki, Y. (1985). "Extraction of polyphenols from *Pinus radiata* bark," *Holzforschung* 39(5), 267-271. DOI: DOI: 10.1515/hfsg.1985.39.5.267

Yesil-Celiktas, O., Otto, F., and Parlar, H. (2009). "A comparative study of flavonoid contents and antioxidant activities of supercritical CO_2 extracted pine barks grown in different regions of Turkey and Germany," *European Food Research and Technology* 229(4), 671-677. DOI: 10.1007/s00217-009-1101-5

Zhang, L. L., and Lin, Y. M. (2008). "HPLC, NMR, and MALDI-TOF MS analysis of condensed tannins from *Lithocarpus glaber* leaves with potent free radical scavenging activity," *Molecules* 13(12), 2986-2997. DOI: 10.3390/molecules13122986

Zhang, L.-L., Lin, Y.-M., Zhou, H.-C., Wei, S.-D., and Chen, J.-H. (2010). "Condensed tannins from mangrove species *Kandelia candel* and *Rhizophora mangle* and their antioxidant activity," *Molecules* 15(1), 420-431. DOI: 10.3390/molecules15010420

Zhang, R., Li, L., and Liu, J. (2015). "Synthesis and characterization of ferric tannate as a novel porous adsorptive-catalyst for nitrogen removal from wastewater," *RSC Advances* 5(51), 40785-40791.

Zhao, X. D., Cheng, Y. F., Fan, W., Vladimir, C., Volha, V., and Alla, T. (2014). "Inhibitive performance of a rust converter on corrosion of mild steel," *Journal of Materials Engineering and Performance* 23(11), 4102-4108. DOI: 10.1007/s11665-014-1199-x

Zhishen, J., Mengcheng, T., and Jianming, W., (1999). "The determination of flavonoid contents in mulberry and their scavenging effects on superoxide radicals," *Food Chemistry* 64(4), 555-559. DOI: 10.1016/S0308-8146(98)00102-2

Article submitted: April 5, 2019; Peer review completed: June 3, 2019; Revised version received: June 21, 2019; Accepted: June 24, 2019; Published: July 9, 2019.
DOI: 10.15376/biores.14.3.6863-6882